

A Competitive Flow Cytometry Screening System for Directed Evolution of Therapeutic Enzyme

Feng Cheng,[†] Tsvetan Kardashliev,^{†,‡} Christian Pitzler,[†] Aamir Shehzad,^{†,||} Hongqi Lue,[§] Jürgen Bernhagen,[§] Leilei Zhu,^{*,†} and Ulrich Schwaneberg^{*,†,‡}

[†]Lehrstuhl für Biotechnologie, RWTH Aachen University, Worringerweg 3, 52074 Aachen, Germany

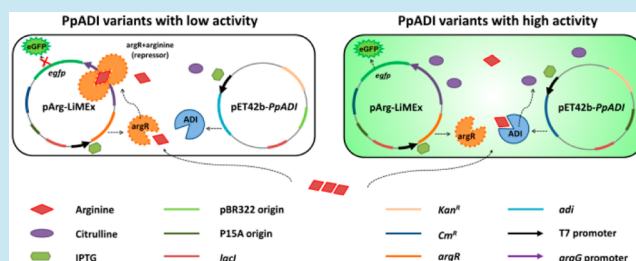
[‡]DWI-Leibniz Institute for Interactive Materials, Forckenbeckstraße 50, 52056 Aachen, Germany

[§]Institute of Biochemistry and Molecular Cell Biology, University Hospital Aachen, RWTH Aachen University, Pauwelsstraße 30, 52074 Aachen, Germany

S Supporting Information

ABSTRACT: A ligand-mediated *eGFP*-expression system (LiMEx) was developed as a novel flow cytometry based screening platform that relies on a competitive conversion/binding of arginine between arginine deiminase and arginine repressor. Unlike product-driven detection systems, the competitive screening platform allows to evolve enzymes toward efficient operation at low substrate concentrations under physiological conditions. The principle of LiMEx was validated by evolving arginine deiminase (ADI, an anticancer therapeutic) for stronger inhibition of tumor growth. After screening of $\sim 8.2 \times 10^6$ clones in three iterative rounds of epPCR libraries, PpADI (ADI from *Pseudomonas plecoglossicida*) variant M31 with reduced $S_{0.5}$ value (0.17 mM compared to 1.23 mM (WT)) and, importantly, increased activity at physiological arginine concentration (M31: 6.14 s^{-1} ; WT: not detectable) was identified. Moreover, M31 showed a significant inhibitory effect against SK-MEL-28 and G361 melanoma cell lines. ($IC_{50} = 0.02 \mu\text{g/mL}$ for SK-MEL-28 and G361).

KEYWORDS: protein engineering, directed evolution, synthetic biology, competitive screening system, arginine deiminase, LiMEx



Directed evolution is a powerful approach to tailor biocatalysts for industrial and therapeutic applications.^{1,2} One major challenge in directed evolution experiments is the establishment of high-throughput screening systems for efficient coverage of the generated sequence space.³ Traditional screening approaches in agar and microtiter plates typically enable the analysis of 10^4 – 10^5 variants, which is still several orders of magnitude below the size of random mutagenesis libraries (10^8 – 10^9).³ Flow cytometry has emerged as a powerful technology in directed evolution by enabling a throughput of up to 10^7 events per hour.⁴ A key requirement for identifying improved enzyme variants by flow cytometry is the availability of fluorescent reporter systems with sufficient sensitivity and specificity. In a majority of cases, flow cytometry based screening systems employ fluorogenic substrates² or coupling to secondary reaction(s) to generate a fluorescence signal proportional to the specific enzymatic activity.⁴

Recently, product-driven, transcription factor-based biosensors have been integrated in flow cytometry based screening systems for genomic screening,⁵ enzyme evolution^{6,7} and isolation of catabolic genes from metagenome libraries.⁸ The employed transcription factors are regulated by product formation or accumulation within the host organism, which in turn triggers the expression of a fluorescent protein.⁹ The generated fluorescence signal correlates to product formation

within millimolar (mM) concentrations.⁵ However, such concentrations are 1 order of magnitude higher than those of many metabolites in living cells or in blood plasma (e.g., in blood, [arginine] = $\sim 100 \mu\text{M}$).¹⁰ Therefore, it is essential to develop new flow cytometry based screening systems to reengineer enzymes by directed evolution for *in vivo* applications in which the substrate concentration is at micromolar (μM) level.

Here, we demonstrate a flow cytometry based screening system for the detection of subtle differences in intracellular concentrations of metabolites. The described ligand-mediated *eGFP*-expression system (LiMEx) establishes a competitive relationship between the regulation of a fluorescent protein expression (e.g., *eGFP*) by an effector molecule (e.g., arginine) and the biochemical depletion of the effector by a coexpressed recombinant enzyme (e.g., arginine deiminase). The signal intensity derived from the fluorescent protein therefore serves to quantify enzymatic performance. The arginine-based LiMEx (termed Arg-LiMEx) described herein as a prototypic example is derived from the regulation of arginine biosynthesis in *Escherichia coli*, which synthesizes arginine from citrulline by employing argininosuccinate synthetase (ASS) and argininosuccinate lyase (ASL)¹¹ (Figure 1a, green box). The transcription of

Received: July 10, 2014

Published: February 6, 2015

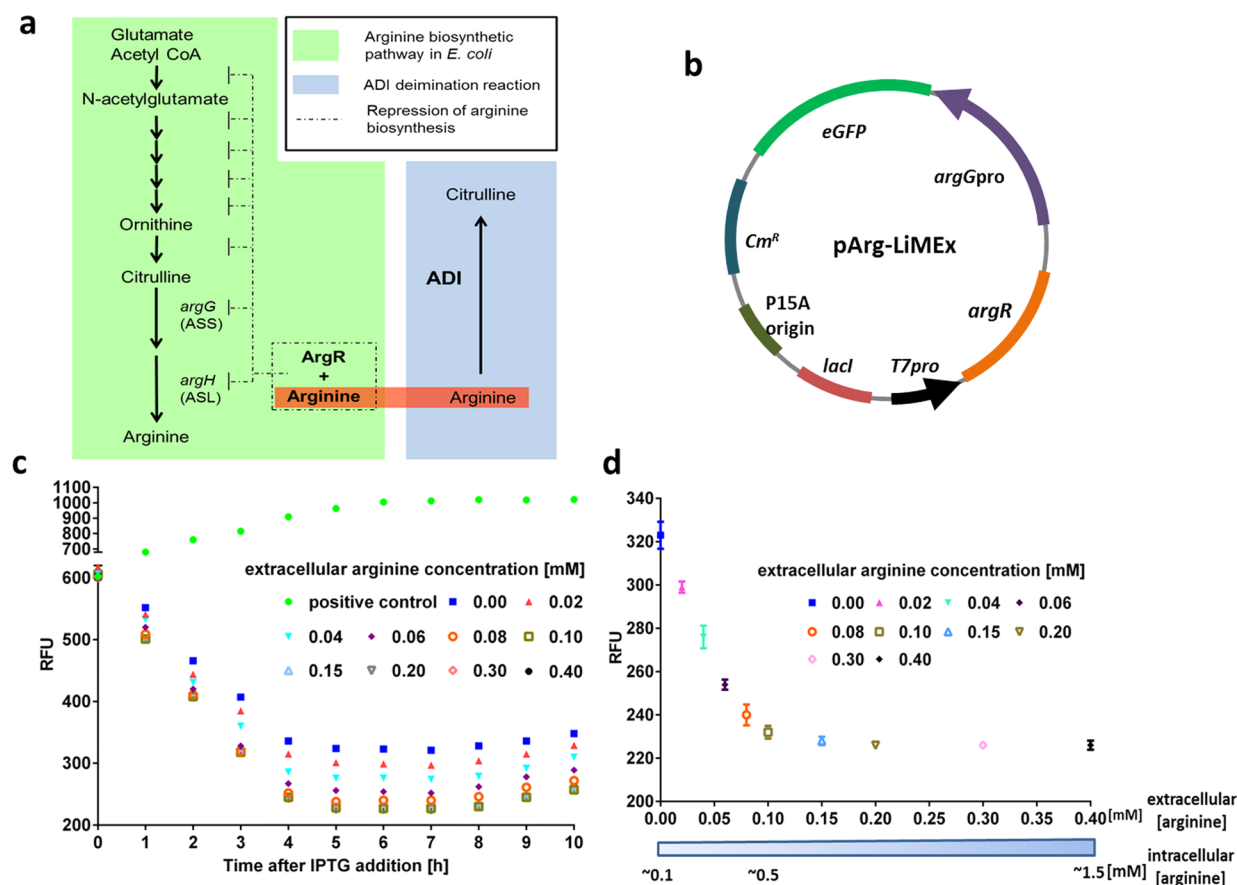


Figure 1. Principle and characterization of eGFP-based arginine sensor encoded by pArg-LiMEX. (a) Schematic outline of the arginine biosynthetic pathway in *E. coli* (green box), the ADI deimination reaction (blue box) and the role of arginine which is the coligand for ArgR and ADI (red box). (b) The pArg-LiMEX vector encodes the Arg-LiMEX for quantifying arginine at micromolar concentrations (100 to 500 μM) in cells. The pArg-LiMEX vector comprises an *ArgR* under the control of a T7 promoter and an *eGFP* gene under the regulation of an *argG* promoter. (c) The fluorescence intensity of noninduced and IPTG-induced *E. coli* cells harboring pArg-LiMEX ($\text{OD}_{600} = 0.6$). Cells were grown in arginine-free media supplemented with varying concentrations of arginine (from 0 to 0.4 mM). Prior to IPTG induction, eGFP was constitutively produced under the control of the *argG* promoter. Fluorescence intensities of induced *E. coli* cells gradually decreased over time and in response to arginine concentrations. The fluorescence intensity of the positive control (noninduced, no ArgR expressed) increased until ~ 6 h after IPTG addition (~ 9 h cultivation time). (d) Fluorescence intensities of induced cells in media with varied concentrations of arginine (from 0 mM to 0.4 mM; time point 6 h after IPTG addition). A decrease in fluorescence was observed between 0 and 0.1 mM arginine.

argG (which encodes ASS) is modulated by the arginine repressor (ArgR). With arginine as corepressor, ArgR tightly binds to the *argG* promoter region^{12,13} and efficiently suppresses eGFP expression (*egfp* under the control of *argG* promoter). Therefore, eGFP fluorescence can be correlated to intracellular arginine concentration, which is determined by the performance of a coexpressing arginine metabolizing enzyme, in this example, arginine deiminase from *Pseudomonas plecoglossicida*^{14,15} (PpADI) (Figure 1a, blue box). We monitored the PpADI activity under physiological conditions ($[\text{arginine}] \sim 0.1$ mM, $\text{pH} \sim 7.4$ and 37°C) by recording eGFP fluorescence intensity of single cells. The Arg-LiMEX screening platform was validated by three iterative rounds of directed evolution in which PpADI was subjected to high mutational loads ($\sim 92\%$ inactive variants; ~ 5 nucleotide exchanges per gene). The final variant (PpADI M31) showed a significantly improved catalytic performance under physiological conditions ($\text{M31}: 6.14 \text{ s}^{-1}$; WT: not detectable) and an augmented inhibitory effect against human melanoma tumor cell lines (IC_{50} (M31) = $0.02 \mu\text{g}/\text{mL}$ for SK-MEL-28 and G361; IC_{50} (WT) = 8.19 (SK-MEL-28) and 4.48 (G361) $\mu\text{g}/\text{mL}$).

The pArg-LiMEX vector (Figure 1b) was designed as a biosensor for quantification of arginine at micromolar concentrations. The biosensor comprises *argR* gene (encoding a repressor protein) under the control of a T7 promoter and *egfp* gene under the control of an *argG* promoter; ArgR serves to regulate *argG* promoter function and, consequently, eGFP expression. IPTG and arginine concentrations are the two extrinsic factors that can modulate the expression level of eGFP. Therefore, an experiment was performed to determine the IPTG concentration at which eGFP expression was altered solely by subtle changes in arginine concentration. *E. coli* cells transformed with pArg-LiMEX were grown in arginine-rich media and the magnitude of fluorescence signal (generated by eGFP) were monitored over time (Figure S1, Supporting Information). In the time prior to ArgR expression, eGFP accumulated and the fluorescence signal of *E. coli* cells increased to ~ 600 RFU. After induction of the *argR* expression by varied concentrations of IPTG (0 to 800 μM), an IPTG concentration-dependent fluorescence signal decrease was observed. A maximal repression of eGFP was achieved when $\geq 100 \mu\text{M}$ IPTG was employed (Figure S1a), and the highest expression level of ArgR was obtained by induction with 0.4 mM IPTG (Figure S1b). To

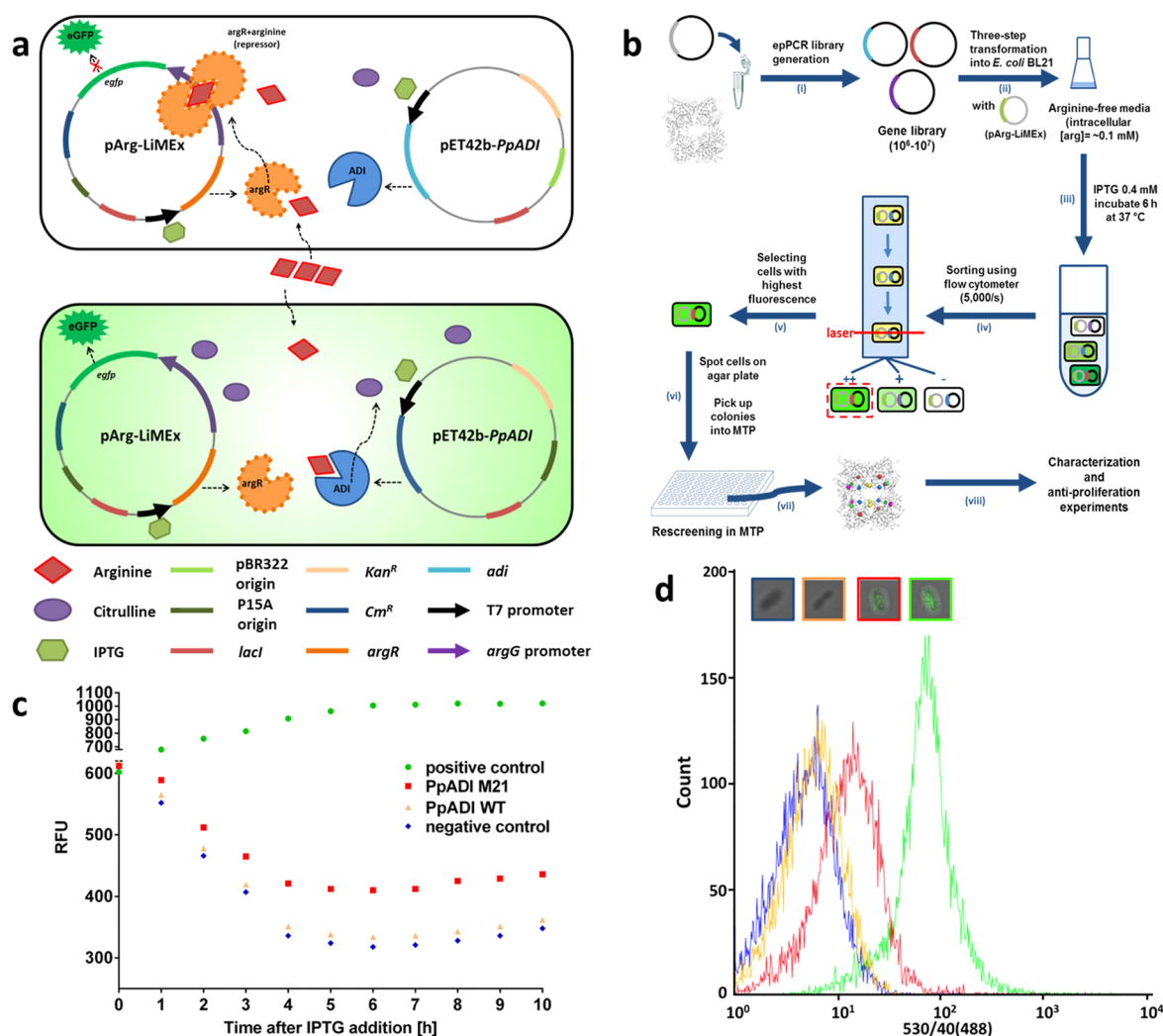


Figure 2. Arg-LiMEx ultrahigh-throughput screening system. (a) Detection principle of the Arg-LiMEx system. eGFP fluorescence depends on intracellular arginine concentration which is determined by PpADI's performance in converting arginine. Top panel: eGFP expression is inhibited when the *argG* promoter is blocked in the presence of arginine by the ArgR-arginine-ArgR complex. Bottom panel: eGFP is produced when PpADI can efficiently deplete the intracellular arginine. (b) The procedure of directed PpADI evolution: (i) mutant library generation by epPCR; (ii) transformation of mutant library into *E. coli* cells with the reporter pArg-LiMEx; (iii–v) prescreening of PpADI mutant library with the Arg-LiMEx system using flow cytometer; (vi) rescreening of PpADI variants in 96-well MTPs; (vii, viii) identification and characterization of improved PpADI variants. (c) Fluorescence intensities show that PpADI M21 can be distinguished from PpADI WT using LiMEx in MTP. Positive control (green) performed with noninduced *E. coli* cells harboring pArg-LiMEx (no ArgR expressed). Negative control (blue) performed with *E. coli* cells harboring pArg-LiMEx and EV (no ADI expression). (d) Flow cytometry analysis of four populations and their distribution (negative control (blue), ADI WT (yellow), ADI M21 (red) and positive control (green)). Images on top show overlays (transmission and fluorescence images) of *E. coli* cells that were recorded by confocal microscopy.

ensure a robust performance, 400 μ M IPTG was selected in further experiments. Notably, although the host strain, *E. coli* BL21(DE3) (genotype: *E. coli* B F⁻ ompT gal dcm lon hsdSB(r_B^- mB⁻) λ (DE₃)), contains endogenous ArgR, the expression level of endogenous ArgR repressor was not sufficient to effectively repress the production of eGFP in the presence of 100 μ g/mL arginine (ArgR should be >31% of total protein amount; Figure S1b).

The applicability of Arg-LiMEx for transforming a given intracellular metabolite concentration into an optical output was initially tested by investigating the relationship between arginine concentration and eGFP fluorescence intensity. *E. coli* cells were transformed with pArg-LiMEx (Figure 1b) and grown in arginine-free media supplemented with varying concentrations of arginine (from 0 to 0.4 mM). In the time prior to ArgR expression, eGFP accumulated, thus the fluorescence signal of *E.*

coli cells increased over time to \sim 600 RFU. The time of induction was used as reference time point (0 h) in Figure 1 and 2. After induction of ArgR expression, a distinct arginine concentration dependent decrease of fluorescence signal was observed after \sim 2 h, whereas the fluorescence signal of the positive control (no IPTG addition; no ArgR expressed) continued to increase (Figure 1c). The most pronounced differences in fluorescence intensity between induced and noninduced samples were observed after 6 h (Figure 1c). The linearity of fluorescence signal was maintained for extracellular arginine concentrations between 0 and 0.1 mM (Figure 1d), corresponding to an intracellular concentration range of \sim 0.1–0.5 mM (calculated on the basis of ref 11); a range that adequately covers the arginine level in blood plasma (100–120 μ M). eGFP derived fluorescence did not decrease further at extracellular arginine concentrations \geq 0.1 mM. These values are consistent with

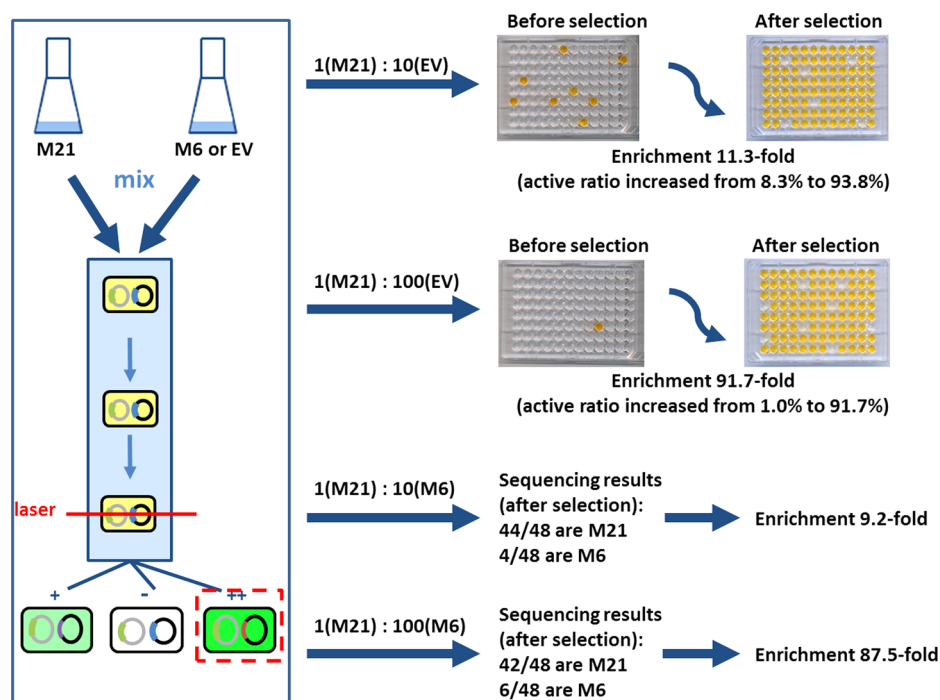


Figure 3. Determination of enrichment factors of four model populations based on citrulline detection assay or Sanger sequencing of the variants obtained from library sorting. The EV and PpADI M21 were grown separately in arginine-free media, harvested (6 h after IPTG induction), mixed at a ratio of 1:10 or 1:100 (M21:EV) and subjected to flow cytometric analysis and sorting. Citrulline generated by PpADI M21 was detected by measuring the yellow product (A_{490}) formed in the citrulline assay. Similarly, PpADI M6 and M21 were mixed at ratios of 1:10 and 1:100, respectively, and Sanger sequencing was employed for the detection of enrichment factors.

published *in vitro* studies of ArgR inhibition strength.¹³ Another experiment performed to test the change in ArgR expression level over time showed that the expression level of ArgR was not affected by varying arginine concentration (0–0.4 mM arginine) (Figure S2b). In addition, no significant changes in cell growth rates were observed as a result of the varied arginine concentrations (Figure S2a) which is likely because the arginine is a nonessential amino acid for *E. coli*. These results indicated that the weak repression of eGFP expression at 0 mM arginine was neither due to lower expression rates of ArgR nor was caused by different cellular growth rates (when there is 0 mM arginine in the growth media, there is ~ 0.1 mM arginine in the *E. coli* cells, on the basis of ref 11). The low intracellular arginine concentration will lead to low repression of GFP. Taken together, the preliminary tests indicated that the monitoring of physiological arginine concentration (arginine concentration: 100–120 μ M; pH ~ 7.4) is feasible with the pArg-LiMEx.

The aforementioned findings prompted us to develop a pArg-LiMEx based ultrahigh-throughput screening system for screening PpADI variants with improved activity under physiological conditions (e.g., pH: ~ 7.4 and arginine concentration: 100–120 μ M). The connection between competitive arginine binding, conversion and fluorescent read out of the Arg-LiMEx is shown in Figure 2a, and the screening strategy is outlined in Figure 2b. First, the influence of IPTG concentration on fluorescence intensity of eGFP was tested in 96-well microtiter plate (Figure S3); 400 μ M IPTG led to the most significant difference in fluorescence intensity between PpADI WT and M21 after 6 h induction (Figure 2c) and highest overexpression of ArgR. Therefore, 400 μ M IPTG was used in all follow-up experiments. Next, in order to establish flow cytometry sorting parameters, a comparison of four populations (negative control, PpADI wild type (WT, $k_{\text{cat}} = 0.18 \text{ s}^{-1}$), PpADI M21 ($k_{\text{cat}} = 18.27 \text{ s}^{-1}$; ~ 100 -

fold higher k_{cat} than WT), positive control) was analyzed by flow cytometry (6 h after IPTG induction) (Figure 2d). Cells cotransformed with pArg-LiMEx and pET (“empty vector” EV, no ADI insert) and noninduced *E. coli* cells harboring pArg-LiMEx served as negative and positive controls, respectively. The negative control (no PpADI expressed) had the lowest mean fluorescence value ($F_{\text{mean}} = 7$; calculated from 10 000 events) and the positive control (no ArgR expressed) exhibited the highest mean fluorescence value ($F_{\text{mean}} = 90$) (Figure 2d). In the Arg-LiMEx screening host, the expression of PpADI WT resulted in a mean fluorescence value of 8 (slightly above the negative control due to its low activity), while PpADI M21 yielded a mean fluorescence value of 19 (10 000 events) (Figure 2d). M21’s higher mean value than the WT, and the distinct shift of its populations, indicated that more active PpADI variants can be distinguished by flow cytometry analysis.

Enrichment factors were determined by sorting model populations comprising mixtures of *E. coli* cells harboring either PpADI M21 or empty vector (EV). The EV and PpADI M21 were grown separately in arginine-free media, harvested (6 h after IPTG induction), mixed at a ratio of 1:10 or 1:100 (M21:EV) and subjected to flow cytometric analysis and sorting. *E. coli* cells harboring PpADI M21 were well separated from the negative control (EV; no ADI) by the P1 gate which captured 0.01% of the negative control (EV) and 9.6 or 1.2% of the model populations (1:10 or 1:100; Figure 3). Sorted cells were grown onto agar plates and transferred into MTPs for detailed quantification of activity employing the reported citrulline quantification assay.¹ The enrichment factors of the two sorted model populations, 11.3-fold (the active/inactive ratio from 8.3 to 93.8%) and 91.7-fold (from 1.0 to 91.7%), validated the Arg-LiMEx screening system with the selected sorting gate (Figure 3). Additionally, we performed sorting of model populations comprising mixtures of

Table 1. Kinetic Constants of PpADI WT, Parent M21 and the “Best” Variant M31

	k_{cat} [s^{-1}]	$S_{0.5}$ [mM]	$k_{\text{cat}}/S_{0.5}$ [$\text{mM}^{-1}\cdot\text{s}^{-1}$]	ν (s^{-1}) at [arginine] = 100 μM
WT	0.20 \pm 0.02	1.23 \pm 0.16	0.16	n.d. ^a
M21	18.27 \pm 0.23	0.33 \pm 0.02	55.36	2.64 \pm 0.19
M31	26.37 \pm 0.66	0.17 \pm 0.02	155.12	6.14 \pm 0.13

^an.d.: no conversion detected.

PpADI M6 ($k_{\text{cat}} = 11.64 \text{ s}^{-1}$) and PpADI M21 ($k_{\text{cat}} = 18.27 \text{ s}^{-1}$) at ratios of 1:10 and 1:100, respectively. The enrichment factors of the two sorted model populations, from sequencing results, were 9.2-fold (PpADI M21: PpADI M6 = 1:10) and 87.5-fold (PpADI M21: PpADI M6 = 1:100), respectively. These results further indicated that the Arg-LiMEx screening system is able to distinguish between PpADI variants with 1.6-fold difference in k_{cat} value.

PpADI M21 was employed as a parent variant for validation of the Arg-LiMEx screening platform in three iterative rounds of directed evolution (89–92% inactive variants; mutation frequency of ~ 5 nucleotide exchanges per gene) using the procedure outlined in Figure 2 and the stringent gate P1 during sorting by flow cytometry (Figure S4). In essence, M21 was generated after screening 9300 clones in four rounds of evolution in a time span of 3 years. Three rounds of evolution (in total 8.2 million variants) were performed to generate M31 by Arg-LiMEx within six months. PpADI activity was detected in $\sim 90\%$ of all sorted cells, and $\sim 30\%$ of the sorted populations showed at least a 1.5-fold improvement compared to the parent M21. The two variants (M22 and M23) that exhibited the highest activities ($\nu_{\Delta c}$) at 100 μM arginine (Table S1) in the initial evolution round were selected as templates for the second round of evolution, and the variants M24, M25, and M26 were chosen for the third round of directed evolution. After the third round of directed evolution, four variants (M27 to M30) were isolated, sequenced and subjected to kinetic characterization using crude cell extracts. All four PpADI variants contained unique mutations and not only improved catalytic rate but reduced $S_{0.5}$ (“ K_M ”) values as well (Table S1). Variant M27 (M21+E39G/F42Y/V293I) was further reengineered by introducing the beneficial amino acid substitutions (namely, N74S, K312R, R288H, T193A, E134G, E136G, D215E and F163S) identified in three rounds of epPCR (Figure S5) (k_{cat} and $S_{0.5}$ values in Table S1). Finally, PpADI M31 (M21+V293I/F42Y/E39G/K312R/T193A/R288H/E134G/E136G) was identified as the most improved PpADI variant with significantly reduced $S_{0.5,\text{app}}$ values (0.17 mM) and increased catalytic activity ($\nu_{\Delta c,\text{app}} = 3.096 \mu\text{M}\cdot\text{s}^{-1}$) at physiological arginine concentrations (100 μM arginine) (Table S1).

Kinetic characterization of three purified PpADIs (PpADI WT, PpADI M21 (parent), and PpADI M31) (Table 1) were performed under conditions that mimic blood plasma environment (~ 0.1 mM arginine, PBS buffer pH 7.4:137 mM NaCl, 2.7 mM KCl, 10 mM Na_2HPO_4 , 2 mM KH_2PO_4). M31 exhibited the lowest $S_{0.5}$ value (0.17 mM), the highest k_{cat} value (26.37 s^{-1}), the highest enzymatic efficiency (k_{cat}/K_M) (155.12 $\text{mM}^{-1}\cdot\text{s}^{-1}$; 2.8-fold higher than parent M21 and 969.5-fold higher than WT), and most significantly the highest reported activity at 100 μM arginine ($\nu_{\text{M21}} = 2.64 \text{ s}^{-1}$, $\nu_{\text{M31}} = 6.14 \text{ s}^{-1}$) (Table 1).

Two arginine-auxotrophic human melanoma cell lines (SK-MEL-28 and G361) were selected to evaluate the *in vitro* antiproliferation activity of M31. The half-maximal inhibitory concentrations (IC_{50}) of M31, PpADI WT and M21 were determined (WT: 8.19 $\mu\text{g}/\text{mL}$ for SK-MEL-28 and 4.48 $\mu\text{g}/\text{mL}$

for G361; M21: 0.06 $\mu\text{g}/\text{mL}$ for SK-MEL-28 and 0.07 $\mu\text{g}/\text{mL}$ for G361; M31: 0.02 $\mu\text{g}/\text{mL}$ for SK-MEL-28 and G361). In summary, M31 exhibited the lowest IC_{50} value against the SK-MEL-28 (0.02 $\mu\text{g}/\text{mL}$; 0.24% of WT) and G361 (0.02 $\mu\text{g}/\text{mL}$; 0.45% of WT) cell lines (Table S2) and displayed a strong inhibition effect even at a low enzyme dosage (0.08 $\mu\text{g}/\text{mL}$, Figure S6). IC_{50} values of the reported ADI (MhADI from *Mycoplasma hominis*) have been determined in the context of melanoma cell proliferation and PpADI M31 showed a five times lower IC_{50} value than the commercial MhADI (0.1 $\mu\text{g}/\text{mL}$ toward G361).¹⁶ In comparison to other therapeutic enzymes, e.g., the recombinant human arginase (in phase II clinical trials for hepatocellular carcinoma (HCC)),¹⁷ PpADI M31 displays a 21-fold lower IC_{50} value for the SK-MEL-28 cell line (PpADI M31: 0.02 $\mu\text{g}/\text{mL}$; rhArg: 0.42 $\mu\text{g}/\text{mL}$).¹⁷

To illustrate the versatility of Arg-LiMEx for screening arginine converting enzyme variants with reduced K_M value/improved activity at low arginine concentration, we additionally analyzed two populations of Co-hArgI (Co²⁺ as cofactor for human arginase I; $K_M = 0.19$ mM) and Mn-hArgI (Mn²⁺ as cofactor for human arginase I; $K_M = 2.33$ mM)¹⁸ by the Arg-LiMEx screening system using flow cytometry. Figure S7b showed the two populations of Co-hArgI (the pink curve in Figure S7) and Mn-hArgI (the orange curve in Figure S7). The Co-hArgI in Arg-LiMEx system resulted in a mean fluorescence value of 43 RFU, which was 2.1-fold higher than that of Mn-hArgI (a mean fluorescence value of 21 RFU). These results were in a good agreement with the colorimetric assay data in which Co-hArgI showed ~ 2.3 times higher activity than Mn-hArgI under the physiological conditions (0.76 vs 0.33 of A_{530}). Furthermore, a stringent gate P2 was set up in the statistical analysis, which captured 0.01% events of Mn-hArgI and 8.7% of Co-hArgI. Moreover, an analysis of the events being inside the gate P2 shows that $>99\%$ events are Co-hArgI (Figure S7). Taken together, the above results indicated that Arg-LiMEx platform can distinguish arginases with ~ 2 -fold difference in activity toward ~ 0.1 mM arginine (arginine concentration in the expression host *E. coli* when there is no external arginine supply).

In summary, Arg-LiMEx represents a novel generation flow cytometry based screening platform for the identification of arginine metabolizing enzymes at low arginine concentrations that amply reflect physiological conditions. Arg-LiMEx biosensor differs from the existing product-driven flow cytometry based screening systems in its mode of regulation of reporter's expression and possible applications. In product-driven screening systems, the generated fluorescence signal is proportional to product formation; i.e., when the concentration of product is very low, the fluorescence signal is also low compared to the signal obtained when the product concentration is high. It could lead to unreliable detection when the transcription factor has low response to the product. In LiMEx, a reverse proportionality was established. The decrease of the ligand/substrate concentration translates into the gain of fluorescence signal (Figure 1d). This is due to the biosensor's design wherein a competition between the metabolite's enzymatic depletion and its role in the regulation of

reporter expression governs the magnitude of the output signal. Therefore, LiMEx offers a novel concept for screening of enzymes for efficient *in vivo* conversion of substrates at low concentration (μM range). For example, this Arg-LiMEx platform could be used for identification of improved arginases (powerful therapeutics against arginine-auxotrophic HCCs and melanomas,¹⁷ as shown in the previous paragraph), and nitric oxide synthases (applied for vascularized tumors¹⁹). Furthermore, the competitive selection principle of LiMEx is not limited to arginine and can very likely be extended to other metabolites or compounds in which a repressor is activated at a low concentration. Some therapeutic enzymes that could be conceptually evolved *via* LiMEx are shown in Table S3, for example, asparaginase, a drug for treatment of leukemia,²⁰ could be evolved by an “Asp-LiMEx system” based on a competition between L-asparagine operon repressor (AnsR) and asparaginase toward asparagine (physiological concentration ~ 0.1 mM).

METHODS

All chemicals were of analytical grade or higher quality and were purchased from Sigma-Aldrich (Steinheim, Germany) and Applichem (Darmstadt, Germany); all enzymes were purchased from New England Biolabs (Frankfurt, Germany) or Fermentas (St.Leon-Rot, Germany), unless stated otherwise. Glutamic dehydrogenase (GDH) was purchased from Sigma-Aldrich. Plasmid extraction and PCR purification kits were purchased from Macherey-Nagel (Düren, Germany). Microtiter plates (flat bottom transparent MTP, flat bottom black MTP and v-bottom transparent MTP) were purchased from Greiner Bio-One (Frickenhausen, Germany).

Construction of Arginine Biosensor Plasmid pArg-LiMEx. Plasmid pArg-LiMEx (Figure S8) was constructed by introducing *argR*, *argG* and *eGFP* in pACYCDuet vector. First, high-fidelity PCR amplifications of *argR*, *argG* and *eGFP* were carried out according to the reaction and thermocycling conditions outlined in Tables S4 and S5 using the plasmid templates pDB169 (*argR*), pDIA539 (*argG*) and pEGFP (*eGFP*) and the respective primer pairs $\text{argR}_{\text{fwd}}/\text{argR}_{\text{rev}}$, $\text{argGPro}_{\text{fwd}}/\text{argGPro}_{\text{rev}}$ and $\text{eGFP}_{\text{fwd}}/\text{eGFP}_{\text{rev}}$ (Table S6). The primers were designed to introduce unique combinations of restriction sites to each amplified fragment. In the case of *argR* amplification, a T7 terminator sequence between the gene's complementary sequence and the 3'-end restriction site was included in the respective reverse primer as well. Next, *argR* fragment with *NcoI* site at its 5'-end and a *BamHI* site at the 3'-end was introduced in pACYCDuet by restriction cloning to obtain pACYCDuet-*argR*.^{12,21} pACYCDuet-*argR*-*argGPro* was constructed by introducing the *argG* promoter (*argGPro*) DNA fragment in pACYCDuet-*argR* using restriction cloning and *BamHI*/*EcoRI* cloning sites. Finally, *eGFP* fragment was inserted into pACYCDuet-*argR*-*argGPro* using *EcoRI*/*HindIII* restriction sites to form the arginine biosensor plasmid, pArg-LiMEx. Restriction digestion and ligation were carried out according to the manufacturer's recommendations and chemically competent *E. coli* DH5 α cells (New England Biolabs, Frankfurt, Germany) were used for the propagation of the intermediate and final genetic constructs.

Expression Strains and Media. *E. coli* BL21-Gold (DE3) cells (Invitrogen, Karlsruhe, Germany) were used as host strain for all expression experiments. Cells harboring pArg-LiMEx were grown in 250 mL Erlenmeyer flasks in a rotary shaker (INFORS HT, USA) at 37 °C, 250 rpm in arginine-free medium¹³ (M9 minimal medium supplemented with glucose (0.05% instead of

0.5%) and a mixture of all proteinogenic amino acids (0.005% of each) except for L-arginine) or medium supplemented with varied concentrations of arginine. Coexpression²² of ArgR (pArg-LiMEx-borne) and ADI (pET42a-borne) was carried out in the aforementioned media supplemented with chloramphenicol (34 $\mu\text{g}/\text{mL}$) and kanamycin (50 $\mu\text{g}/\text{mL}$) to maintain the presence of both plasmids over proliferation cycles.

Characterization of pArg-LiMEx. *E. coli* BL21-Gold (DE3) cells harboring pArg-LiMEx were grown in arginine-free media supplemented with varied concentrations of arginine (0, 0.02, 0.04, 0.06, 0.08, 0.1, 0.15, 0.2, 0.3 and 0.4 mM). IPTG was added as an inducer to cultures after cell density (OD_{600}) reached 0.6. The overall fluorescence ($\lambda_{\text{ex}} = 480$ nm; $\lambda_{\text{em}} = 505$ nm; gain 140) in flat bottom black MTP was measured using Tecan Infinite M1000 Pro MTP reader (Tecan Group AG, Zürich, Switzerland) hourly after the adjustment of cell density (OD_{600} equal 0.6).

Optimization of LiMEx and Identification of Sorting Parameters for Flow Cytometry. BD Influx cell sorter (BD Biosciences, San Jose, CA) was used for cell analysis and sorting. The flow cytometer was fitted with a 100 μm nozzle and PBS was used as a sheath fluid. A sample of cells with pArg-LiMEx was diluted in ice-cold PBS buffer to an optical density below 0.1 and immediately analyzed and sorted according to the scatter characteristics (forward and side scatter) as well as to the fluorescence signal excited at 488 nm and emitted at a bandpass filter at 530/40 nm. Cells were sorted with speed of 5000 events/s allowing a throughput of 1.8×10^7 events/h. During sorting, single cells were spotted onto LB_{kan/cm} agar plates and then incubated later (37 °C for 12–14 h) until colonies formed.

An optimized three-step transformation method was employed for introducing pArg-LiMEx and pET42b (+) into *E. coli* BL21-Gold (DE3). First, the pArg-LiMEx was transformed into chemical competent *E. coli* BL21-Gold (DE3) cells to obtain *E. coli* BL21-Gold (DE3)/pArg-LiMEx. Second, competent cells of *E. coli* BL21-Gold (DE3)/pArg-LiMEx were prepared employing the Hanahan method.²³ In the third step, competent *E. coli* BL21 Gold (DE3)/pArg-LiMEx cells were transformed with pET42b-ADI M21 or pET42b (empty vector). A single colony from each cell type was used to inoculate arginine-free media (37 °C). After reaching an OD_{600} value of 0.6, IPTG at final concentration of 0.4 mM was added and expression was carried for 6 h at 37 °C. *E. coli* cells harboring pET42b-PpADI M21 or pET42b were mixed with ratios of 1:10, and 1:100 (M21:EV; OD_{600} value ratios) as model libraries and then subjected to flow cytometry sorting as described in the previous paragraph.

Protein Expression and Preparation of Crude Cell Extracts in 96-Well Microtiter Plate (MTP). Cultivation and expression of *E. coli* BL21-Gold (DE3)/pArg-LiMEx/pET42-PpADI in 96-well plates (v-bottom, transparent) were performed as previously described.¹⁰ Cell lysis was performed by the addition of 80 μL lysozyme (final concentration: 80 $\mu\text{g}/\text{mL}$) to each well of MTP containing frozen cell pellet. The cell pellet was resuspended by pipetting up and down and subsequently incubated at 37 °C for 20 min. After centrifugation at 4000 rpm for 15 min (Eppendorf centrifuge 5804, Hamburg, Germany), the clarified supernatant was used for activity assays.

Citrulline-Detection System in MTP Format.¹ Cell lysate (20 μL) of *E. coli* BL21-Gold (DE3)/pArg-LiMEx/pET42-PpADI was transferred into 96-well MTP (flat bottom, transparent). The arginine conversion by PpADI was initiated by the addition of arginine solution (1 mM, pH 7.4, PBS buffer), and the mixture was incubated (20 min, 37 °C). Next, acid-ferric solution¹⁰ (60 μL) and diacetyl monoxime (DAM, 20 μL , 0.5 M)

were added for citrulline detection. The reaction mixture was incubated for 30 min at 55 °C. Absorbance was measured at 490 nm using a MTP reader (Tecan Sunrise, Tecan Group AG, Zürich, Switzerland).

Ammonia-Detection System in MTP Format.¹⁵ Cell lysate (20 μ L) of *E. coli* BL21-Gold (DE3)/pArg-LiMEx/pET42-PpADI was transferred into 96-well MTP (flat bottom, transparent) which were supplemented with 80 μ L detection reagent (0.4 mM NADH, 5 mM α -ketoglutarate, and 5.55 U GDH) into each well, and the assay plates were incubated at 37 °C for 5 min. The cascade reaction was initiated by the addition of 100 μ L of arginine solution (0.1 mM, pH 7.4, PBS buffer) and the absorbance at 340 nm was recorded by using a microtiter plate reader (Tecan Sunrise, Tecan Group AG, Zürich, Switzerland). The Beer–Lambert law was used for calculating the ammonia production velocity ($v_{\Delta c}$) as previously described.¹⁵

PpADI Error-Prone PCR (epPCR) Library Generation and Cloning. Three high error-rate epPCR libraries (with 0.15 mM Mn^{2+}) were generated using the Mastermix and thermocycling conditions outlined in Table S4, Table S7, and Table S8. The gene encoding PpADI M21 (K5T/K30R/C37R/D38H/D44E/A128T/G129S/L148P/V291L/E296 K/H404R) was used as a template for the first round.¹⁵ For the generation of the following rounds of epPCR library, the plasmids encoding 2 to 4 PpADI variants exhibiting the highest activity identified in the previous round of epPCR library were isolated, mixed at equimolar ratio and used as templates. The purified epPCR products were cloned into pET42b(+) vector by MEGA-WHOP²⁴ employing the reaction conditions outlined in Table S9.

DpnI digested MEGAWHOP products were transformed into NEB 5-alpha electrocompetent *E. coli* cells (New England Biolabs, Frankfurt, Germany) and cells were spread onto LB_{kan} agar plates (transformation efficiency >10⁹ CFU/mL). On the following day, the plasmid libraries were isolated from the colonies and transformed into *E. coli* BL21-Gold (DE3)/pArg-LiMEx (prepared by transforming pArg-LiMEx in *E. coli* BL21 gold (DE3) and making the resulting strain competent using the Hanahan method²³ (transformation efficiency >10⁸ CFU/mL)).

Site-Directed Mutagenesis for Recombination of Selected Amino Acid Positions. Site-directed mutagenesis of the PpADI at amino acid positions 74, 134, 136, 163, 193, 215, 288, and 312 was performed as previously described.¹⁵ Variants with recombined substitutions (identified in the three epPCR rounds) were generated using PpADI M27 as template (identified from the third epPCR library) using PCR protocol and primers outlined in Table S10 and Table S11, respectively. The resulting PCR product was purified by using a PCR purification kit then digested with *DpnI* and transformed into *E. coli* BL21-Gold (DE3).¹⁴

Expression and Purification of PpADI WT, Parent M6 and the “Best” Variant M31. PpADI WT, PpADI M21 and variant PpADI M31 were expressed in shaking flasks and purified by anion-exchange chromatography (TOSOH, Stuttgart, Germany). PD-10 columns (GE Healthcare, Darmstadt, Germany) were subsequently used for desalting as previously described.¹⁰ Protein concentrations after the final purification step were measured using the Thermo Scientific Pierce BCA protein assay kit (Rockford, IL, USA).

Kinetic Characterization of the Purified PpADI Variants. The initial velocity was obtained using the ammonia detection assay (37 °C, purified PpADI (0.1–1.8 mM); final substrate solution (0.5 mM to 10 mM of arginine, PBS buffer, pH

7.4). The data were fitted to the sigmoidal model of kinetics eq 1 (in which v is the initial velocity, v_{\max} is the maximum velocity, $[S]$ is the substrate concentration, $S_{0.5}$ is the ligand concentration producing half occupation, and h is the Hill coefficient) by using GraphPad Prism software (GraphPad software, San Diego, CA, USA). The k_{cat} was calculated from the ratio of V_{\max} and enzyme concentration.

$$v = \frac{v_{\max} \times [S]^h}{S_{0.5}^h + [S]^h} \quad (1)$$

Cultivation Conditions for Melanoma Cell Line Cultures. Two melanoma cell lines, SK-MEL-28 and G361, were cultivated at 37 °C, 5% CO₂ in DMEM medium (Life Technologies, Darmstadt, Germany) supplemented with 10% fetal calf serum (FCS), nonessential amino acids (1 \times), pyruvate (1 \times), 100 μ g/mL streptomycin, and 100 μ g/mL penicillin.

Cell Proliferation Assay. 180 μ L growth medium containing $\sim 2.5 \times 10^3$ melanoma cells were added to each well of a 96-well MTP. Twenty microliters of purified and sterile PpADI (0.1–10 μ g/mL, PpADI WT, M21, and M31) were added into the growth medium after SK-MEL-28 and G361 cells had been grown for 24 h. The MTP plates were incubated for 6 days at 37 °C in an incubator containing 95% air and 5% CO₂. Quantitative cell proliferation assays were performed using the CellTiter-Blue dye (Promega, Mannheim, Germany) as previously described.¹⁵ The concentration of PpADI enzymes required for 50% inhibition of the cells in culture was defined as the IC₅₀, and IC₅₀ values were determined by using GraphPad Prism 6 (GraphPad Software, Inc., San Diego, CA). All values are expressed as mean \pm SD.

Gene Synthesis, Expression and Activity Analysis of Human Arginase I. The hArgI gene was codon-optimized for expression in *E. coli* and synthesized by MWG Operon (Ebersberg, Germany). The synthetic hArgI gene was cloned into pET42b using restriction cloning with NdeI/XhoI sites. The final construct of pET42b-hArgI was transformed into chemically competent *E. coli* BL21 Gold (DE3)/pArg-LiMEx for further protein expression and activity detection.

E. coli cells harboring pET42b-hArgI and pArg-LiMEx were grown at 37 °C in arginine-free media to an OD₆₀₀ of 0.6. IPTG (0.4 mM, final concentration) and 100 μ M CoCl₂ (for Co-hArgI) or MnSO₄ (for Mn-hArgI) were added into the media, respectively, and cells were grown for further 6 h at 37 °C with shaking (250 rpm). *E. coli* cells with Co-hArgI or Mn-hArgI were subjected to flow cytometry analysis respectively as described in a previous paragraph (Optimization of LiMEx and Identification of Sorting Parameters for Flow Cytometry). Additionally, the activity of arginase from cell lysate was detected by a colorimetric assay developed by Archibald.²⁵

■ ASSOCIATED CONTENT

📄 Supporting Information

This material is available free of charge via the Internet at <http://pubs.acs.org>.

■ AUTHOR INFORMATION

Corresponding Authors

*Tel: +49-241-80-24170. Fax: +49-241-80-22578. E-mail: u.schwaneberg@biotec.rwth-aachen.de.

*Tel: +49-241-80-20675. Fax: +49-241-80-22578. E-mail: l.zhu@biotec.rwth-aachen.de.

Present Address

^{||}Department of Biotechnology and Genetic Engineering, Kohat University of Science and Technology, Pakistan.

Author Contributions

F.C., L.Z. and A.S. designed the experiments. F.C., C.P. and H.L. performed experiments. F.C. and C.P. analyzed the data. F.C. and T.K. wrote the manuscript. L.Z., J.B. and U.S. conceived and directed the project and revised the manuscript. All authors commented on the manuscript.

Notes

The authors declare no competing financial interest.

ACKNOWLEDGMENTS

We thank Dr. Daniel Charlier (Laboratorium voor Erfelijkheidsleer en Microbiologie, Vrije Universiteit Brussel, Belgium) for supplying the plasmid pDB169 harboring *ArgR*, Dr. Evelyne Krin (Institut Pasteur, Unité Génétique des Génomes Bactériens, France) for providing the *argG* promoter gene in pDIAS30 plasmid, and Dr. Anett Schallmeyer (TU Braunschweig, Germany) for providing the pACYCDuet-1 plasmid. We also thank Dr. Ronny Martinez and Dr. Ran Tu for valuable discussions and Ms. Kristin Rübsum for performing confocal microscope measurements. F.C. is supported by a Ph.D. scholarship from China Scholarship Council (2011833152). C.P. is supported by a grant from the Federal Ministry of Education and Research (BMBF) (FKZ 031A165). This work was supported through funds from RWTH Aachen University, the DWI-Leibniz Institute for Interactive Materials, and Chinese Academy of Sciences Visiting Professorships for Senior International Scientists (Y3J8041101) to U.S., and by a grant from Uniklinik RWTH Aachen START program (Molecular Tumor Markers; no. 696055) to J.B..

REFERENCES

(1) Zhu, L., Verma, R., Roccatano, D., Ni, Y., Sun, Z. H., and Schwaneberg, U. (2010) A potential antitumor drug (arginine deiminase) reengineered for efficient operation under physiological conditions. *ChemBioChem* 11, 2294–2301.

(2) Ruff, A. J., Dennig, A., Wirtz, G., Blanusa, M., and Schwaneberg, U. (2012) Flow cytometer-based high-throughput screening system for accelerated directed evolution of P450 monooxygenases. *ACS Catal.* 2, 2724–2728.

(3) Yang, G. Y., and Withers, S. G. (2009) Ultrahigh-throughput FACS-based screening for directed enzyme evolution. *ChemBioChem* 10, 2704–2715.

(4) Dietrich, J. A., McKee, A. E., and Keasling, J. D. (2010) High-throughput metabolic engineering: Advances in small-molecule screening and selection. *Annu. Rev. Biochem.* 79, 563–590.

(5) Binder, S., Schendzielorz, G., Stabler, N., Krumbach, K., Hoffmann, K., Bott, M., and Eggeling, L. (2012) A high-throughput approach to identify genomic variants of bacterial metabolite producers at the single-cell level. *Genome Biol.* 13, R40.

(6) Schendzielorz, G., Dippong, M., Grunberger, A., Kohlheyer, D., Yoshida, A., Binder, S., Nishiyama, C., Nishiyama, M., Bott, M., and Eggeling, L. (2014) Taking control over control: Use of product sensing in single cells to remove flux control at key enzymes in biosynthesis pathways. *ACS Synth. Biol.* 3, 21–29.

(7) Siedler, S., Schendzielorz, G., Binder, S., Eggeling, L., Bringer, S., and Bott, M. (2014) SoxR as a single-cell biosensor for NADPH-consuming enzymes in *Escherichia coli*. *ACS Synth. Biol.* 3, 41–47.

(8) Uchiyama, T., Abe, T., Ikemura, T., and Watanabe, K. (2005) Substrate-induced gene-expression screening of environmental metagenome libraries for isolation of catabolic genes. *Nat. Biotechnol.* 23, 88–93.

(9) Schallmeyer, M., Frunzke, J., Eggeling, L., and Marienhagen, J. (2014) Looking for the pick of the bunch: High-throughput screening of

producing microorganisms with biosensors. *J. Curr. Opin. Biotechnol.* 26C, 148–154.

(10) Zhu, L., Tee, K. L., Roccatano, D., Sonmez, B., Ni, Y., Sun, Z. H., and Schwaneberg, U. (2010) Directed evolution of an antitumor drug (arginine deiminase PpADI) for increased activity at physiological pH. *ChemBioChem* 11, 691–697.

(11) Caldara, M., Dupont, G., Leroy, F., Goldbeter, A., De Vuyst, L., and Cunin, R. (2008) Arginine biosynthesis in *Escherichia coli*—Experimental perturbation and mathematical modeling. *J. Biol. Chem.* 283, 6347–6358.

(12) Van Duyne, G. D., Ghosh, G., Maas, W. K., and Sigler, P. B. (1996) Structure of the oligomerization and L-arginine binding domain of the arginine repressor of *Escherichia coli*. *J. Mol. Biol.* 256, 377–391.

(13) Krin, E., Laurent-Winter, C., Bertin, P. N., Danchin, A., and Kolb, A. (2003) Transcription regulation coupling of the divergent *argG* and *metY* promoters in *Escherichia coli* K-12. *J. Bacteriol.* 185, 3139–3146.

(14) Zhu, L., Cheng, F., Piatkowski, V., and Schwaneberg, U. (2014) Protein Engineering of the Antitumor Enzyme PpADI for Improved Thermal Resistance. *ChemBioChem* 15, 276–283.

(15) Cheng, F., Zhu, L., Lue, H. Q., Bernhagen, J., and Schwaneberg, U. (2015) Directed arginine deiminase evolution for efficient inhibition of arginine-auxotrophic melanomas. *Appl. Microbiol. Biotechnol.* 99, 1237–1247.

(16) Ensor, C. M., Holtsberg, F. W., Bomalaski, J. S., and Clark, M. A. (2002) Pegylated arginine deiminase (ADI-SS PEG(20,000) (mw)) inhibits human melanomas and hepatocellular carcinomas *in vitro* and *in vivo*. *Cancer Res.* 62, 5443–5450.

(17) Cheng, P. N. M., Lam, T. L., Lam, W. M., Tsui, S. M., Cheng, A. W. M., Lo, W. H., and Leung, Y. C. (2007) Pegylated recombinant human arginase (rhArg-peg(5,000mw)) inhibits the *in vitro* and *in vivo* proliferation of human hepatocellular carcinoma through arginine depletion. *Cancer Res.* 67, 309–317.

(18) Stone, E. M., Glazer, E. S., Chantranupong, L., Cherukuri, P., Breece, R. M., Tierney, D. L., Curley, S. A., Iverson, B. L., and Georgiou, G. (2010) Replacing Mn(2+) with Co(2+) in human arginase I enhances cytotoxicity toward L-arginine auxotrophic cancer cell lines. *ACS Chem. Biol.* 19, 333–342.

(19) Zheng, P. P., Hop, W. C., Luider, T. M., Smitt, P. A. E. S., and Kros, J. M. (2007) Increased levels of circulating endothelial progenitor cells and circulating endothelial nitric oxide synthase in patients with gliomas. *Ann. Neurol.* 62, 40–48.

(20) Broome, J. D. (1981) L-Asparaginase: discovery and development as a tumor-inhibitory agent. *Cancer Treat. Rep.* 65, 111–114.

(21) Lim, D. B., Oppenheim, J. D., Eckhardt, T., and Maas, W. K. (1987) Nucleotide sequence of the *argR* gene of *Escherichia coli* K-12 and isolation of its product, the arginine repressor. *Proc. Natl. Acad. Sci. U. S. A.* 84, 6697–6701.

(22) Tolia, N. H., and Joshua-Tor, L. (2006) Strategies for protein coexpression in *Escherichia coli*. *Nat. Methods* 3, 55–64.

(23) Hanahan, D., Jessee, J., and Bloom, F. R. (1991) Plasmid transformation of *Escherichia coli* and other bacteria. *Methods Enzymol.* 204, 63–113.

(24) Miyazaki, K., and Takenouchi, M. (2002) Creating random mutagenesis libraries using megaprimer PCR of whole plasmid. *Biotechniques* 33, 1033–1034.

(25) Archibald, R. M. (1945) Colorimetric determination of urea. *J. Biol. Chem.* 157, 507–518.